www.jjgastro.com

Journal of Gastroenterology Research and Practice

Research Article

Open Access, Volume 6

Intelligent breath analysis based on SERS sensor for diagnosis of helicobacter pylori and evaluation of clinical therapy effect of HP antibody conjugated lipid loaded with ICG treating HP resistance

Yixin Huang[1]; Wei Wang[1]; Xue Cuili[1]; Fangfang Xia[2]; Binyu Zhu[1]; Weicheng Wang[1]; Jinlei Jiang[1]; Yao Hu[1]; Han Jin[1]; Linjia Peng[2]; Shengsheng Cui[2]; Zhao Qirui[2]; Hui Liang[2]; Ren Zhiguang[2]; Zhe Yu[2]; Lichen Xiang[2]; Jesus M de la Fuente[3]; Wujun Xiong[4]; Dongmei Yang[5]; Lan Zhong[6]; Daxiang Cui[1,2]*

[1]Institute of Nano Biomedicine and Engineering, School of Automation and Sensing, Shanghai JiaoTong University, Shanghai 200240, China.

[2]Institute of Medical and Engineering Cross Integration, Henan Intelligent Diagnosis and Treatment Technology Engineering Center, Henan Zhongzhou Laboratory, The First Affiliated Hospital, Henan University Medical College, Kaifeng 475001, China.

[3]Instituto de Ciencia de Materiales de Aragon (ICMA-CSIC), Universidad de Zaragoza, 50009 Zaragoza, Spain

[4]Department of Gastroenterology, Shanghai Pudong Hospital Affiliated to Fudan University, Shanghai 201399, PR China.

[5]Department of Gastroenterology, Maternal and Child Health Hospital, Lianyungang 222062, PR China.

[6]Department of Gastroenterology, Dongfang Hospital Affiliated to Tongji University, Shanghai 200120, PR China.

***Corresponding Author:** Daxiang Cui
Institute of Nano Biomedicine and Engineering, School of Automation and Sensing, Shanghai JiaoTong University, Shanghai 200240, China.
Email: dxcui@sjtu.edu.cn

Received: Jul 06, 2026
Accepted: Jul 23, 2026
Published: Jul 30, 2026
Archived: www.jjgastro.com

Keywords: Helicobacter pylori; VOC biomarkers; Microfludic chip; SERS sensor; HP drug resistance therapy.

Abstract

Helicobacter Pylori (HP) infection and antibiotic resistance have become serious threat to human health. How to realize precise diagnosis and therapy of HP owns huge clinical requirement. In this study, twelve Volatile Organic Compound (VOC) biomarkers are identified to distinguish patients with positive HP from HP negative healthy persons. Among them, three VOC biomarkers are associated with HP resistance. The breath analysis approach based on Microfludic chip loaded with Surface Enhanced Raman Scattering (SERS) sensor was developed to detect these biomarkers. Fe3O4 nanoparticles and hollow silver microspheres were synthesized and assembled into SERS sensor, and then was integrated into microfludic chip. Exhaled gas from persons were collected by airbags, and then airbag outlet was linked to the microfluidic chip inlet, collected breath gas were automatically absorbed into the microfluidic chip, nine Raman bands associated with the nine biomarkers are selected as standard spectrum to identify HP positive persons in different states, the remaining three biomarkers were associated with HP drug-resistance. The approach has successfully screen HP positive patients with and without antibiotic resistance from crowd. 250 breath samples from clinical patients were diagnosed as HP positive patients with sensitivity of 96.4% and specificity of 100%, 100 HP negative persons with 97.8% sensitivity and 100% specificity. KNN, DT, SVM, ANN models were also established. 10 patients with HP resistance were selected to treat with HP Antibody-conjugated Liposome-coated ICG under ultrasound irradiation for one week, then exhaled gas were collected from 10 patients and examined using microfludic chip sensors to show HP negative.

In conclusion, the 12 VOC biomarkers of HP and breath analysis microfludic chip sensors can screen out effectively HP positive patients with and without drug resistance from person populations, can evaluate treatment effects of HP with and without drug resistance. This system has great potential for clinical translation in near future.

Introduction

Helicobacter Pylori (HP) resides in the human gastric antrum and is a common pathogenic bacterium, is closely associated with various gastrointestinal diseases such as chronic gastritis, peptic ulcers, mucosa-associated lymphoid tissue lymphoma and gastric cancer [1].

Approximately half of the world's population is estimated to be infected with Helicobacter pylori, and the infected population is widespread [2]. Children are often asymptomatic carriers of the infection, and symptoms typically manifest in adult hood [3]. The majority of individuals infected with Helicobacter pylori do not exhibit symptoms but rather act as carriers. The existence of a large number of asymptomatic carriers poses challenges to the prevention and treatment of HP [4,5]. To date, there is no single drug that can completely eradicate HP. Patients with HP infection-related diseases must seek timely medical attention and undergo targeted treatment based on their specific conditions [6].

Up to date, the increasing rates of HP antibiotic resistance and the emergence of multidrug-resistant strains pose significant challenges to its treatment [7,8].

In order to treat HP, my group designed and prepared Oral pH sensitive GNS@ab nanoprobes, animal experiment confirmed that it targeted therapy Helicobacter pylori without disturbance gut microbiome, its therapeutic effects is very good, the nanoprobe is also very safety [9].

My group also developed HP antibody-conjugated liposomes loaded with indocyanine green, animal experiment confirmed that which actively targeted and combined with Helicobacter pylori in gastric tissues, under ultrasound activated, ICG produced singlet oxygen (1O2) to kill Helicobacter pylori. Therapeutic effect is very good [10]. Therefore, timely detection of H. pylori in patients is crucial, as it can effectively reduce the likelihood of further deterioration, including the development of gastric cancer [11,12].

Up to date, there are various diagnostic methods for Helicobacter pylori infection, each own with its advantages and disadvantages [13]. For example, HP diagnostic tests can be performed using both invasive and non-invasive techniques. Examples of invasive techniques include endoscopy, histopathological analysis, rapid urease testing, culture, and PCR detection [14-17]. Non-invasive techniques include serology, fecal antigen testing, and breath tests [18,19]. Currently, the most widely used method is the Urea Breath Test (UBT) [20], is considered the "gold standard" diagnostic method for detecting Helicobacter pylori infection. It exhibits high diagnostic accuracy for detecting H. pylori infection in patients with digestive disorders, which involves patients orally ingesting Carbon-14 labeled urea capsules, HP produced urease to decompose urea into CO_2, and then CO_2 enter the lungs through the bloodstream and are expelled with exhalation. And then detecting their breath to confirm if the C14-isotope and CO_2 existed. If CO_2 existed, the patient is confirmed to be with HP infection.

So far through exhaled Volatile Organic Compound (VOC) detection is a non-labeled detection method, which has advantages such as non-invasiveness, rapid sampling, easy storage, and low cost. Moreover, it does not require patients to eat Carbon-14 labeled urea capsules and has no adverse effects on patients. Therefore, Breath screening tumors and bacteria have become current Trends and Hot Topics [21,22].

My group also screened out 14 VOC biomarkers to distinguish early gastric cancer and advanced gastric cancer and healthy person, developed SERS sensor to realize fast VOC biomarkers detection, established Intelligent Diagnosis Model, realized to screen early gastric cancer patients [23,24]. We also used SERS sensor to realize to screen COVID-19 virus rapidly, also developed microneedle vaccine to treat COVID-19 [25,26]. We also developed phenyl-β-D glucuronide-induced breath analysis to realize pan-cancer detection [27]. This developed SERS sensor to screen early gastric cancer via detecting exhaled VOC biomarkers have finished clinical trial verification.

Therefore, volatile organic compounds in exhaled breath, serving as diagnostic markers for Helicobacter pylori infection, can be applied for the screening of such infections, offering advantages such as being non-labeled, rapid, non-invasive, and cost-effective. In 2011, Agnieszka Ulanowska and colleagues utilized SPME-GC/MS to determine the VOCs in the breath of Helicobacter pylori-positive patients. Differences in the levels of isobutane, 2-butanone, and ethyl acetate were detected between the experimental and control groups [28].

In this study, 12 VOC biomarkers firstly were identified to distinguish HP positive patients from healthy persons by Gas Chromatography−Mass Spectrometry (GC-MS). Meanwhile, a breath analysis approach based on Microfluidic chip with Fe_3O_4-hollow silver microspheres SERS sensor was developed to recognize the different VOC biomarker patterns in both simulated and real breath samples. When the collected breath samples were controlled to enter into the Channel inside microfluidic chip, the Fe_3O_4-hollow silver microspheres sensors adsorbed the VOC biomarkers, under the laser irradiation, SERS spectrometry result was exhibited on the Video screen, the clean

SERS sensor ensured a high selectivity and sensitivity for the identified VOC biomarkers [23,29]. The established approach was used to analyze breath samples with the advantages of safety, non-invasive, simple operation, rapid detection, low cost, and reliability. The VOC biomarkers and breath analysis approach in this work can not only be used to diagnose HP but also be used to Evaluate HP therapy effect, and have great potential in clinical application.

Machine learning has played a crucial role in disease screening and diagnosis in recent years, with common approaches including Support Vector Machine (SVM), Artificial Neural Network (ANN), Logistic Regression (LR), K-Nearest Neighbors (KNN), and Decision Trees (DT) [30]. Genetic-Algorithm-based classification models can handle diverse datasets from different sources, including breath samples, voice signals, computed tomography images, etc [31]. Genetic Algorithm has been applied in the diagnosis of various diseases such as cancer, COVID-19 [26,32], Parkinson's syndrome [33], chronic obstructive pulmonary disease [34], and more. As a powerful classifier, Genetic Algorithm is versatile across disciplines, demonstrating excellent performance even with small datasets [35-38]. This study attempts to use Genetic Algorithm to classify limited data, thereby facilitating the screening of Helicobacter pylori-positive samples. As shown in Scheme1, exhaled breath was input into auto syringe pump, then was absorbed into detection passage in microfludic chip, and then was detected via SERS sensor [39,40,41], detection site included the sensor composed of magnetic nanoparticles and silver microsphere, under laser Irradiation, Raman Scattering Signal was produced based on Sensors interact with exhaled breath, the data was treated via software, display the result of HP positive or HP negative.

We also recruitment 10 patients with HP resistance, and used HP antibody-conjugated liposomes loaded with indocyanine green for oral treating HP resistance, then use microfludic chip sensor to detect VOC biomarkers to evaluate the therapeutic effects.

Therefore, the VOC biomarkers and breath analysis approach in this work can not only be used to diagnose HP but also be used to Judgment HP therapy effect, and have great potential in clinical application.

Experiment section

Ethical statement

All patient experiments were approved by the Ethics Committee of shanghai jiaotong university (No. 2022-322),Clinical trial filing number of the National Medical Products Administration (HUSOM2025-719), Collection of exhaled breath samples from patients with HP and Healthy persons with negative HP were approved by the ethics committees of cooperative hospitals such as First Affiliated Hospital of Henan university (No.2023-019), Pudong Hospital (No.2020-066), Dongfang Hospital (No.2020-122) and Maternal and Child Health Hospital (No.2020-015).

Collection of the breath samples

350 Tedlar bags (SKC Inc., Eighty-Four, PA, USA) were sent to four cooperative hospitals. The breath samples from patients in 25-80 years with positive HP were collected from First Affiliated Hospital of Henan university, Pudong Hospital, Dongfang Hospital; the breath samples from patients in 5-25 years with positive HP were collected from Maternal and Child Health Hospital in Lianyungang. We recruited 350 volunteers from four Hospitals, providing exhaled breath samples, include 250 individuals with Helicobacter pylori infection, some patients among them were with HP resistance, and 100 healthy individuals. None of the volunteers have other malignant tumors, blood disorders and metabolic system diseases. 100 healthy individuals with negative HP were confirmed by hospitals. 250 individuals with H. pylori infection were confirmed through double verification, including a positive result in the carbon-14 breath test and positive bacterial culture from gastric mucosal specimens obtained during gastroscopy. Before breath sample collection, each volunteer was instructed to maintain a natural and calm emotional state within 48 hours and abstain from smoking and drinking alcohol for 24 hours. Demographic information such as age, gender, H. pylori detection values, smoking and drinking history, current medication use, and recent dietary habits were recorded for each volunteer. Within the last hour before sample collection, all volunteers refrained from consuming any food to maintain oral cleanliness. Just before sampling, volunteers rinsed their mouths with pure water. After a 5-minute interval, breath collection began. Before exhaling, volunteers took a deep breath, held it for 3 seconds, and the initial 2-3 seconds of exhalation were not collected. Exhalation was then collected until approximately 80% of a 1-liter Tedlar bag was filled.

Chemical analysis of the breath samples

GC-MS (QP2010 Ultra; Shimadzu) combined with SPME (75 μm CAR/PDMS fiber, Supelco, USA) was used for chemical analysis of the tested breath. The testing process was the same as our previous methods reported [23,26,27].

Preparation of the microfludic chip SERS Sensor

Microfludic chip was prepared by using the same as our previous reported [18]. Magnetic nanoparticles were synthesized by using our reported method [32], silver microsphere was prepared by using reported method [47-49]. Prepared Magnetic nanoparticles and silver microspheres were characterized by TEM and SEM. Magnetic nanoparticles and silver microspheres were mixed and assembled together via self-assembly method, and then were characterized by TEM. The Complex composed of Magnetic nanoparticles and silver microspheres were added into detection channel in microfludic chip, which can realize SERS detection of breath VOC biomarkers. The Prototype machine was established, was composed of microfludic chip SERS Sensor and Raman spectrometer and SERS Analysis software and laser beam and auto syringe pump and CCD and monitor, showed in (Figure S2).

Breath analysis procedure

The breath analysis process based on microfludic chip SERS sensor was as follow [23]:

1) Every Tedlar bag filled with exhaled air was Connected to auto syringe pump, then turn on the switch connected with inlet on the microfludic chip, the exhaled air were Absorbed into Gas detection channel In microfludic chip;

2) Under 785 nm laser Irradiation, sensor composed of Fe3O4 and Silver microsphere adsorbed gas, and then produce raman scattering signal, which enter into CCD device and then were exhibited outside on the Computer display surface.

3) The adsorbed VOC biomarkers on the sensor were

detected within 10 minutes, and then the data were exhibited on the Computer. All measurements were carried out at 25°C.

Statistical analysis

All the results were expressed as mean ± standard deviation (n=3). Statistical significance of obtained results was determined employing the t test and analysis of variance (ANOVA) using SPSS 18.0 software with $p<0.05$ as a minimal level of significance.

Establish machine learning models

In the aforementioned 12 biomarkers, pyridine, formamide, and hexadecanolide had undetectable levels in some samples. To better exclude inherent errors in the detection method, only the remaining 9 organic compounds were selected as reference indicators. The Raman spectra of their standard substances are established. We utilized machine learning techniques, employing MATLAB R2023a (MathWorks, USA), for data classification and prediction, introducing a supervised learning model, Support Vector Machine (SVM), to address the binary classification problem. Prior to modeling, normalization was applied to the high-dimensional data. Support Vector Machine (SVM), Artificial Neural Network (ANN), Logistic Regression (LR), Decision Trees (DT) and K-Nearest Neighbors (KNN) models were established, Genetic Algorithm (GA) was also integrated into the ANN, KNN, DT, SVM models, the performances of integrated models were also evaluated through accuracy, sensitivity, specificity. This allowed for the differentiation between the experimental group and the control group through the analysis of specific VOCs [23,29,50,51].

Clinical experiment of patients with HP drug resistance

10 patients with HP Drug resistance were selected from First Affiliated Hospital of Henan university, and were used for clinical therapy experiments and breath analysis experiments, which was approved by the Ethics Committee of First Affiliated Hospital (2024-171), and were free treatment. Clinical trial approval number of the National Medical Products Administration was permitted (HUSOM2025-719).

In 2020-2021, Oral HP antibody-conjugated liposomes loaded with indocyanine green (Hp Ab-LiP-ICG) were prepared and used to treat HP infected mice, result showed that Hp Ab-LiP-ICG Targeted binding H. pylori, ICG was activated to generate singlet oxygen to eliminate H. pylori under ultrasound irradiation, Hp Ab-LiP-ICG also own high stability and favorable biocompatibility [10]. Based on our previous animal experiment result, we propose to use oral Hp Ab-LiP-ICG nanoprobes to conduct clinical trials to evaluate its HP treatment effectiveness.

The 10 patients were firstly oral HP antibody-conjugated liposomes loaded with indocyanine green, and then used ultrasound to irradiate the patient's stomach to activate ICG to produce ROS to eliminate HP resistance. The therapeutic time is one week, finally collected breath gas via Tedlar bags, then use microfludic chip sensor to detect VOC biomarkers to evaluate the therapeutic effects [23].

Results

The course of microfludic chip SERS sensor used for detection of HP VOC biomarkers and confirm whether exist HP is as shown in Scheme 1.

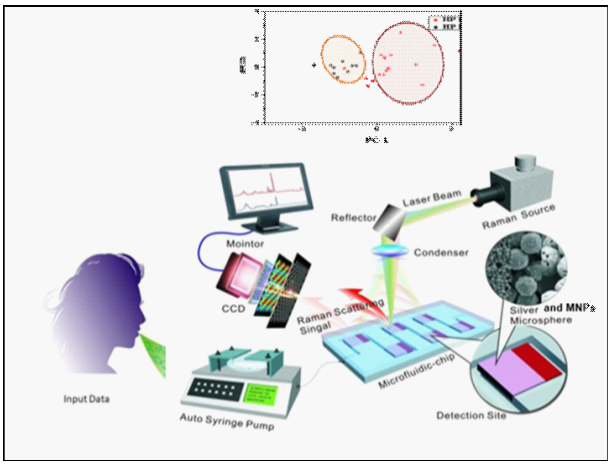

Scheme 1: Schematic illustration of SERS sensor and overview of the processes involved in the breath analysis.

Identification of VOC biomarkers associated with HP

Exhaled breath were collected from Patients with HP positive and healthy persons with HP negative, and then were detected by mass spectrometry and Gas chromatography [23]. The chromatograms of exhaled breath and corresponding Helicobacter pylori infection biomarkers for both infected patients and healthy individuals are illustrated in Figure 1, there existed 12 VOC biomarkers to Distinguish HP positive patients from HP negative persons. The concrete names of 12VOC biomarkers are presented in Table 1.

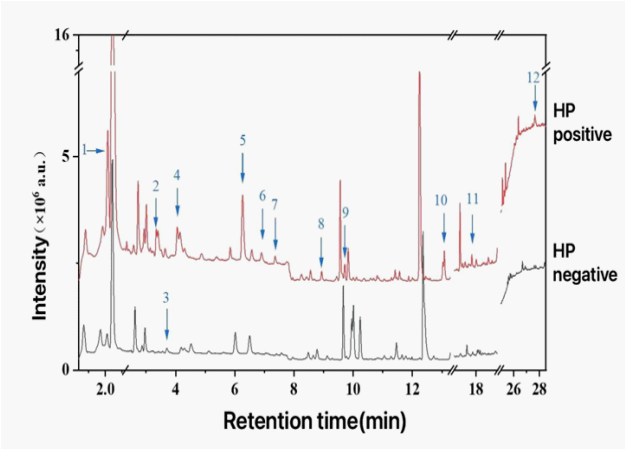

Figure 1: Chromatographic gram of exhaled breath between H. pylori infected patients and healthy persons.

The raman spectra of the eleven VOCs biomarkers of HP

In the aforementioned 12 biomarkers, pyridine, formamide, and hexadecane-1,4-olide had undetectable levels in some samples. Through big data analysis, the three VOC biomarkers are closely associated with HP resistance. Therefore, 1-9 biomarkers were selected to use screen HP positive patients. To better exclude inherent errors in the detection method, only the remaining 11 organic compounds were selected as reference indicators. The Raman spectra of their standard substances are shown in Figure 2. Become No.12 biomarker is associated with HP resistance, therefore, the Raman spectra of No. 12 biomarker Headecane-1,4-lactone was established and shown in Figure S1.

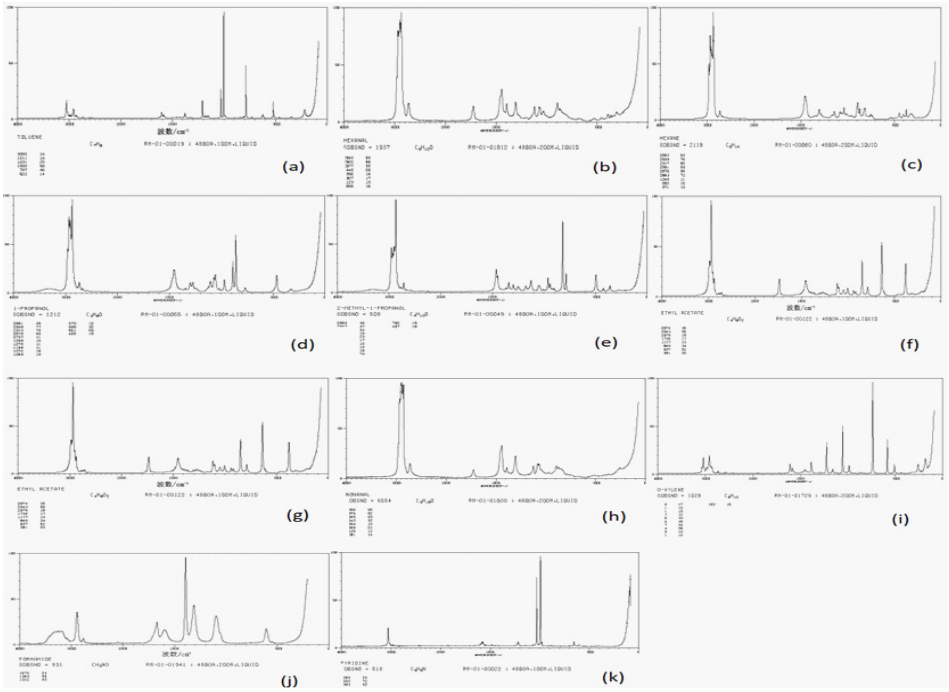

Figure 2: The Raman spectra of the nine VOCs standards of H. pylori. (**A**) Toluene. (**B**) Hexanal. (**C**) Hexane. (**D**) 1-Propanol. (**E**) 2-Methyl-1-Propanol. (**F**) Ethyl acetate. (**G**) Ethyl alcohol. (**H**) Nonanal. (**I**) O-xylene. (**J**) Pyridine. (**K**) Formamide.

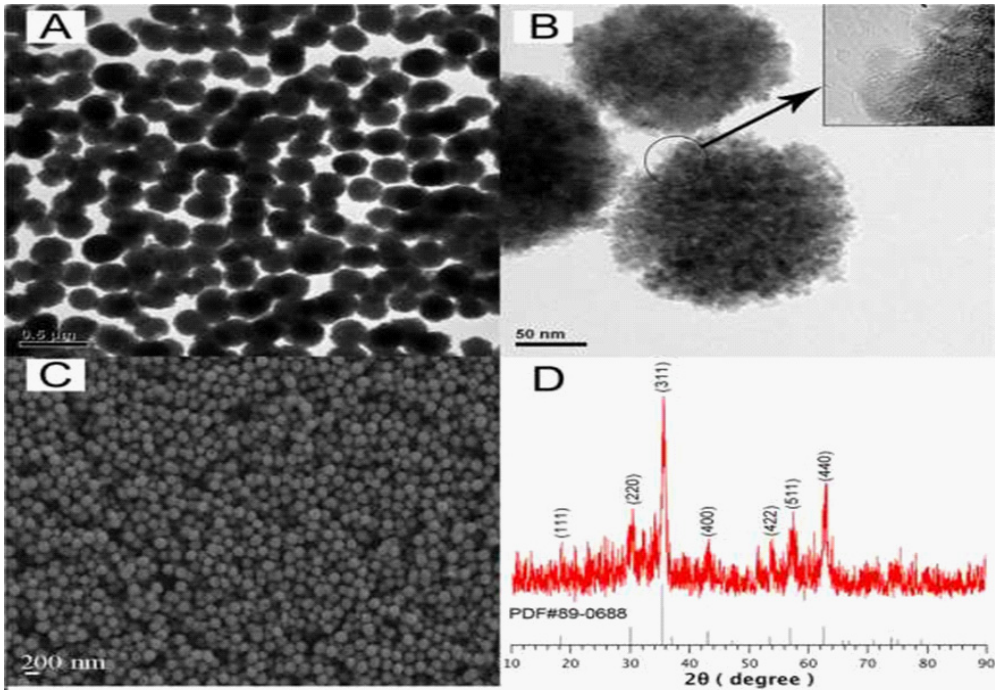

Figure 3: Characterization of Magnetic NPs synthesized in one-pot manner: (A) TEM; (B) HRTEM; (C) SEM; (D) XRD diffraction patterns.

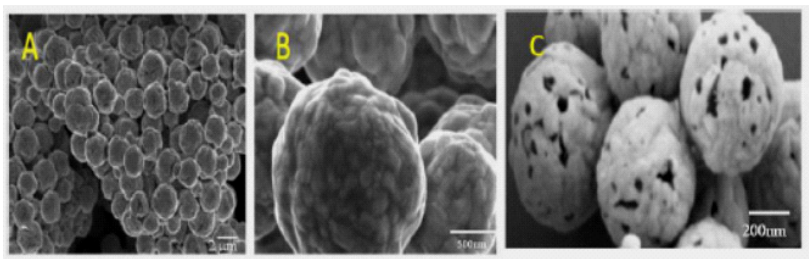

Figure 4: Characterization of Hollow silver microspheres: (**A**) Silver nanoparticles TEM; (**B**) Silver microsphere SEM; (**C**) Hollow silver microsheres SEM.

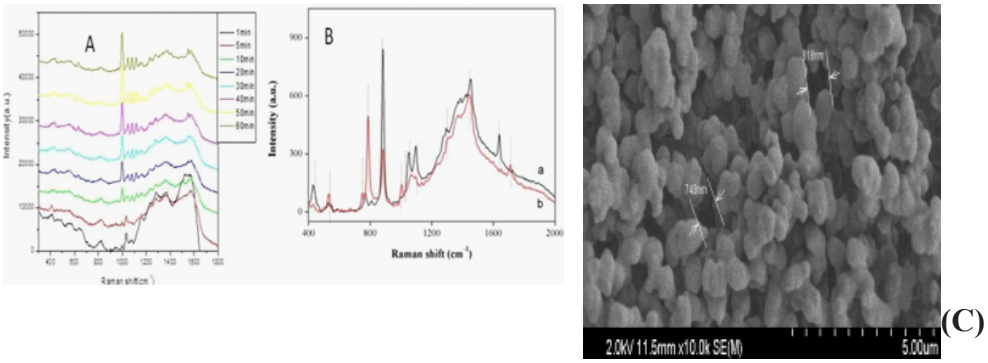

Figure 5: Magnetic nanoparticles integrated into silver microsphere compound (**C**) Integrated compound of MNPs and silver microspheres; (**A**) SERS Raman signals of VOC biomarkers; (**B**) Raman signals of VOC biomarkers.

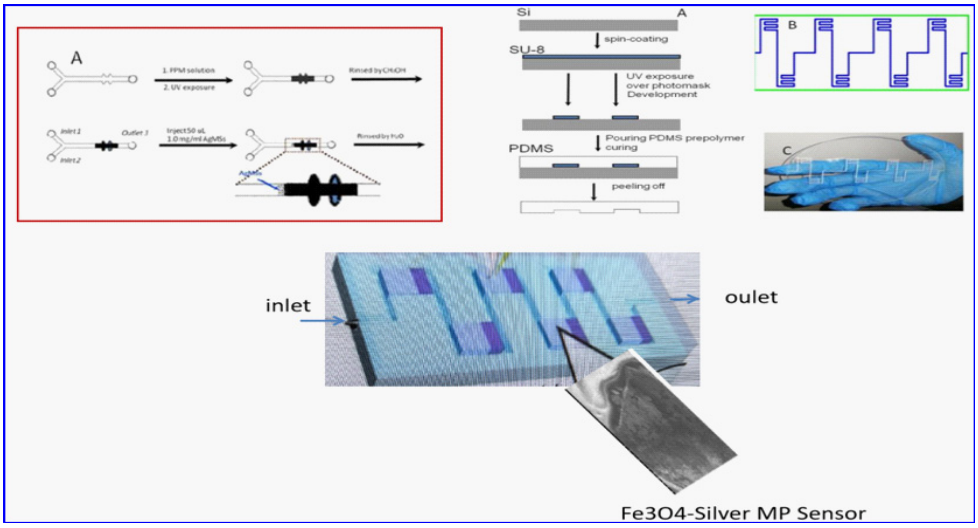

Figure 6: Preparation process of Microfludic chip Sensor with Fe_3O_4 -silver microsphere.

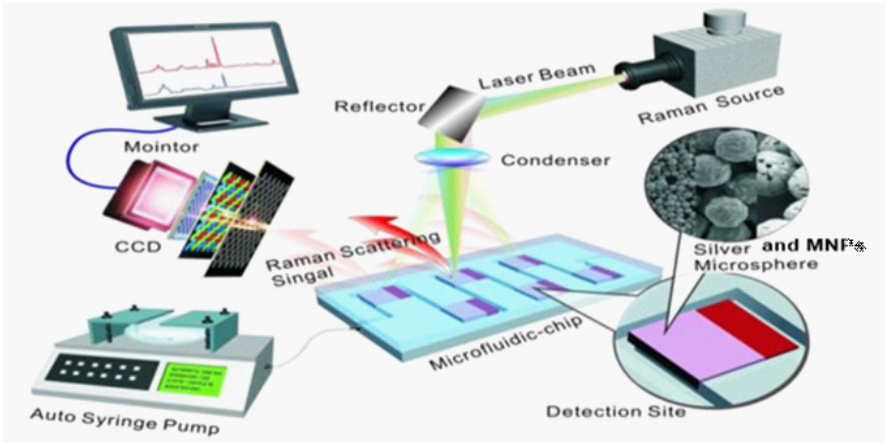

Figure 7: Detection Process of Breath analysis microfludic SERS sensor system for HPVOC.

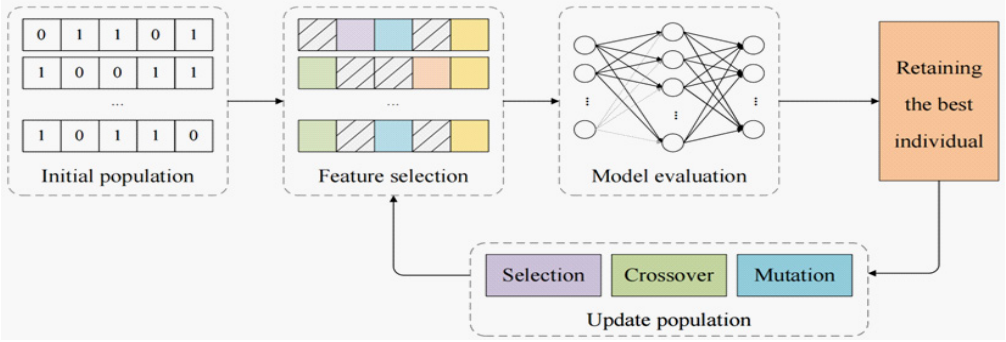

Figure 8: Framework of feature selection based on genetic algorithm and artificial neural network.

Table 1: VOC biomarkers in expiration in HP positive patients.

Peak number	Compound	CAS number
1	n-hexane	110-54-3
2	ethyl acetate	141-78-6
3	2-methyl-1-propanol	75-65-0
4	alcohol	64-17-5
5	toluene	108-88-3
6	1-Propanol	71-23-8
7	hexanal	66-25-1
8	o-xylene	95-47-6
9	Nonanal	124-19-6
10	pyridine	110-86-1
11	formamide	975-12-7
12	Headecane-1,4-lactone	730-46-1

Preparation of microfludic chip with Fe_3O_4-silver microsphere SERS sensor

Our previous studies showed that SERS sensor can increase biomarkers detection sensitivity to 1013 [23], therefore, it is suitable for low concentration biomarkers detection. Nanomaterials such as Magnetic NP, Au and Ag nanoparticles own obvious advantages [42-47], therefore, Magnetic NP and silver microsphere were used to establish microfludic chip SERS sensor.

At first, Magnetic Fe_3O_4 nanoparticles and silver microspheres were prepared and characterized by TEM. As shown in Figure 3, Fe_3O_4 nanoparticles were prepared and characterized [45]. Each magnetic NP is 60 nm scale.

As shown in Figure 4, Silver microsphere were prepared and characterized by using our previous reported technique [48]. Silver microsphere is 200 nm. As shown in Figure 5, magnetic NPs and Silver microspheres were integrated together via self-assembly method in Figure 5C, and then were used as SERS sensor to detect different concentration of VOC biomarker 1-8 samples combined with SERS spectrometer, results showed in Figure 5A and 5B. As shown in Figure 6, Microfludic chip was prepared firstly, then sensor chip composed of Fe3O4-silver microspheres was prepared, input into six sites of detection channel in microfludic chip, finally microfludic chip SERS Sensor with Fe_3O_4 -silver microsphere was successfully prepared, and then was used for detection of VOC biomarkers in Exhaled breath as shown in Figure 7. The finally established microfludic SERS sensor system was shown in Figure S2.

Breath samples analysis Result with microfludic SERS sensor system

Prepared microfludic SERS sensor system was used to detect VOC biomarkers in 350 breath samples. The analysis results of breath samples from HP positive patients and HP negative persons were shown in Table 2. 250 breath samples with HP positive were detected, sensitivity is 96.4%, specificity is 100%. 100 breath samples with HP negative were detected, sensitivity is 97.9%, specificity is 100%.

Table 2: Clinical characteristics of volunteers and analysis results.

Group	No.	Age (years)	Gender (M.F)	Results (%)	
HP Positive	250	(8-70) 39 ± 7.8	150:100	Specificity 100%	Sensitivity 96.4%
HP Negative	100	(10-50) 41 ± 5.8	60:40	100%	97.90%

Artificial intelligence model was established based on analysis data

Using clinical breath gas samples examination data, using Genetic Algorithm (GA) and artificial neural network to establish the intelligence model for diagnosis of HP positive and negative. The framework diagram shown as Figure 8 illustrates a feature selection process based on genetic algorithm and artificial neural network. It starts with the initial population, followed by the feature selection phase. The selected features are then evaluated using an artificial neural network, and the corresponding fitness value is computed. Based on the fitness evaluation, evolutionary operations such as selection, crossover and mutation are applied to generate a new population. This process iterates until an optimal feature subset is obtained.

As shown in Table 3, four kinds of models such as KNN, DT, SVM, ANN were established, and the accuracy and precision, recall and F1 dispalyed different results. ANN + GA model should be best model. As shown in Figure9, the ROC curve is used to evaluate the performance of five classification models, ANN + GA is best model. As shown in Figure 10, it is Confusion matrices for different classifiers. As shown in Figure 11, it is the confusion matrix visualizes the classification performance of four different models. As shown in Figure 12, it is the confusion matrix visualizes the classification performance of four different models.

Table 3: Compares the performance of different machine learning models with and without Genetic Algorithm (GA) optimization.

	Accuracy	Precision	Recall	F1
KNN	0.79	1	0.62	0.77
DT	0.82	0.92	0.75	0.83
SVM	0.89	1	0.81	0.9
ANN	0.93	1	0.88	0.93
KNN+GA	0.86	0.93	0.81	0.87
DT+GA	0.89	0.93	0.88	0.9
SVM+GA	0.93	0.94	0.94	0.94
ANN+GA	0.96	1	0.94	0.97

The evaluation metrics include Accuracy, Precision, Recall, and F1-score. The results indicate that ANN outperforms other models in the baseline scenario, achieving the highest Accuracy (0.93), Recall (0.88) and F1-score (0.93). When optimized with GA, all models show improvement, with ANN+GA achieving the best overall performance: an Accuracy of 0.96, a Precision of 1.00, a Recall of 0.94, and an F1-score of 0.97. These findings suggest that GA optimization enhances model performance, with ANN+GA being the most effective approach.

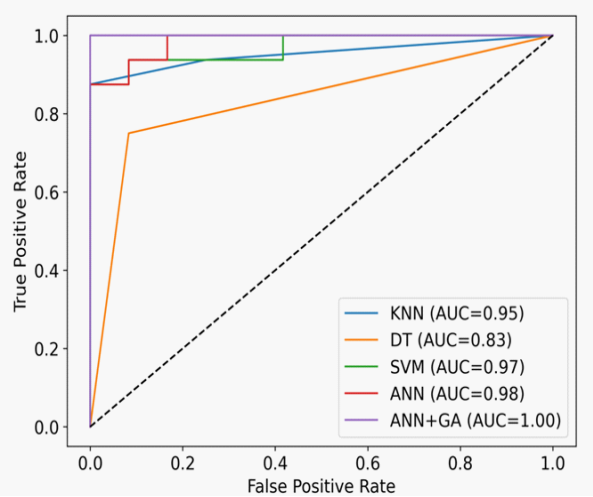

Figure 9: Comparison of ROC curve for different classifiers.

The ROC curve is used to evaluate the performance of five classification models: K-Nearest Neighbors (KNN), Decision Tree (DT), Support Vector Machine (SVM), Artificial Neural Network (ANN), and ANN optimized with a Genetic Algorithm (ANN+GA). The curve depicts the True Positive Rate (TPR) against the False Positive Rate (FPR) for each model. The Area Under the Curve (AUC) serves as a performance metric, where higher AUC values indicate superior classification capability. The ANN+GA model achieves an AUC of 1.00, indicating perfect classification performance, followed by ANN (0.98), SVM (0.97), KNN (0.95), and DT (0.83).

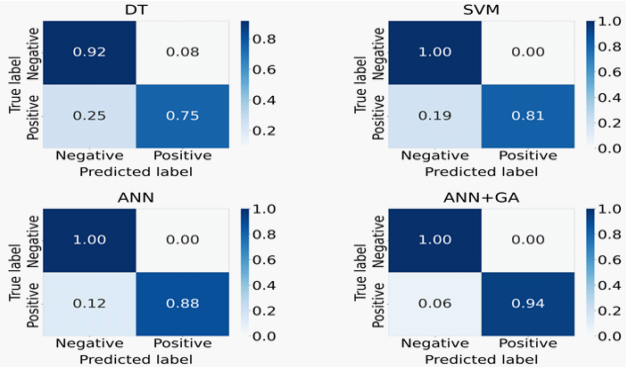

Figure 10: Confusion matrices for different classifiers.

The confusion matrix visualizes the classification performance of four different models: Decision Tree (DT), Support Vector Machine (SVM), Artificial Neural Network (ANN), and ANN with Genetic Algorithm (ANN+GA). Each matrix shows the proportion of correctly and incorrectly classified negative and positive samples. DT has the lowest positive class prediction accuracy, while ANN+GA achieves the best performance with the highest true positive rate (0.94). ANN and SVM also demonstrate strong classification abilities, with ANN+GA outperforming all models.

The box plot illustrates the distribution of feature values after normalization for selected optimal features across two classes: Positive (orange) and Negative (blue). Each box represents the Interquartile Range (IQR) with the median indicated by the horizontal line inside the box. The whiskers extend to 1.5 times the IQR, while individual points outside this range are considered outliers. The differences in distributions between the two classes suggest that these features play a

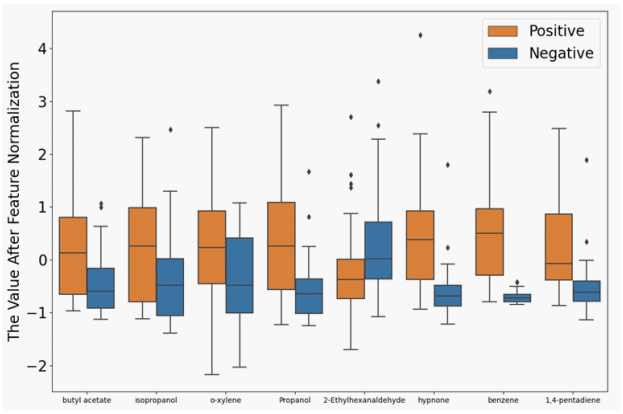

Figure 11: Box plot of the normalized feature values for the selected optimal features.

significant role in distinguishing between positive and negative samples. For example, in the feature "benzene", the values for the Negative class are concentrated around a lower range with minimal variation, whereas the Positive class has a wider distribution with higher median values. This indicates that benzene levels are significantly higher in positive samples compared to negative samples, making it a strong distinguishing feature. Similarly, in the feature "hypnone", the Positive class has a broader and higher distribution than the Negative class, suggesting that higher values of hypnone are more indicative of a positive sample. These differences in distribution patterns highlight the importance of these features in classification.

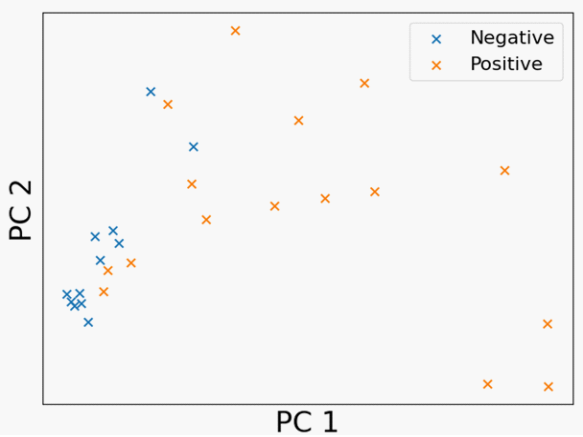

Figure 12: PCA visualization of the test set based on the selected optimal features.

This scatter plot represents a PCA visualization of the test set based on the selected optimal features. The clustering of blue points in the lower-left region and the wider spread of orange points suggest a separation between the two classes along the principal components.

The histogram illustrates the importance of the selected optimal features based on SHAP values, which quantify the average impact of each feature on the model's output. The x-axis represents the mean absolute SHAP value, reflecting the magnitude of each feature's influence on the model's predictions. The y-axis lists the features in descending order of importance. Among these, the feature "Benzene" exhibits the highest SHAP value, indicating it has the greatest impact on the model's decision-making process.

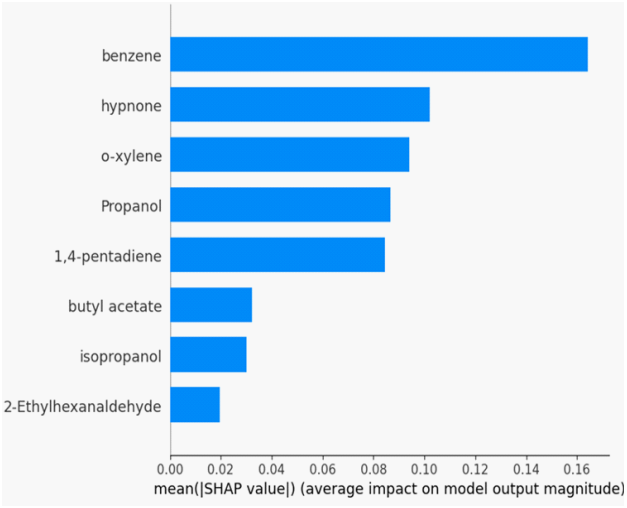

Figure 13: Histogram of feature importance for the selected optimal features, sorted by SHAP value.

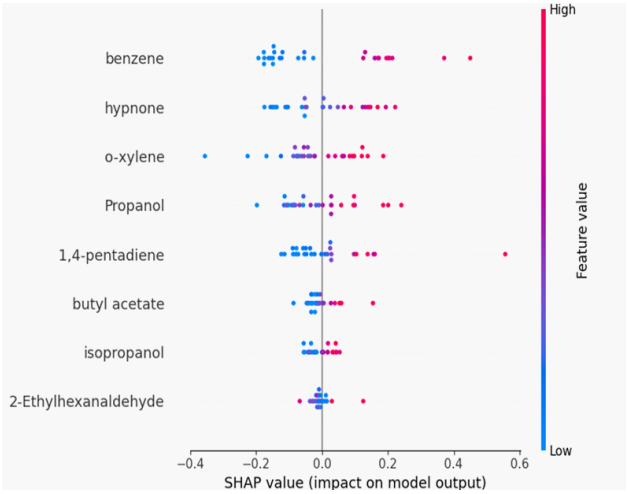

Figure 14: Beeswarm plot of SHAP values for the selected optimal features.

This beeswarm plot visualizes the SHAP values for the selected optimal features, illustrating their impact on the model's predictions. Each dot represents a single data point, with its position on the x-axis showing the SHAP value, indicating whether the feature drives the prediction positively or negatively. The color represents the feature value, with blue indicating lower values and red indicating higher values. Features such as "Benzene" show a strong influence on the model, where higher feature values make the model tend to predict positive and lower feature values make the model tend to predict negative.

Therapy results of 10 patients with HP Drug resistance with HP antibody-conjugated liposome-coated ICG integrated with ultrasound for one week

Compared with patients with HP without drug resistance, patients with HP drug resistance exhibited high Quantity of nonanal, formamide and Headecane-1,4-lactone, On the contrary, patients with HP without drug resistance only exhibited high quantity of Peak number 1 to 9, almost were Zero quantity of peak 10-12 (shown in Table S1). Therefore, peak 10-12 can be used to evaluate whether patients with HP positive exist resistance.

HP Antibody-conjugated Liposome-coated ICG have been used to treat Pig model with HP, treat time is 6 hours, breath screening HP is negative, therapeutic effect is very good [10]. Based on this animal experiment result, we continuously plan to apply for clinical trials to evaluate its therapeutic effects for patients with HP positive. After the clinical trial ethics approval was granted, we selected Ten volunteer patients with HP resistance drug to start clinical treatment experiment with HP Antibody-conjugated Liposome-coated ICG. After 10 patients with HP resistance were treated with HP Antibody-conjugated Liposome-coated ICG under ultrasound irradiation for one week, the breath data showed HP negative as shown in Table S2. Therefore, HP Antibody-conjugated Liposome-coated ICG can be used to treat patients with HP resistance drug, also can be used to treat patients with HP positive without resistance drug.

Discussion

Up to date, Helicobacter pylori has been confirmed to be closely associated with digestive ulcer diseases, chronic active gastroenteritis, Atrophic gastritis and gastric cancer [4]. Epidemiological Investigation on Helicobacter Pylori in Children show that HP infection Significantly affecting growth and development of children [52-54], how to realize precise diagnosis and therapy of HP own great clinical requirement [55]. However, the increasing rates of HP antibiotic resistance and the emergence of multidrug-resistant strains significantly affect the treatment of HP [7,8].

Up to date, examination HP infection have established some widely used methods in clinical practice such as carbon-14 breath test, Blood test for HP antibody, Fecal test for HP antigen [13]. Our group also develop the CCD-based reader combined with CdS quantum dot-labeled lateral flow strips for ultrasensitive quantitative detection of HP CagA [15,16], we also confirmed that differential expression of Phospholipase C Epsilon 1 is associated with gastric cancer and Chronic Atrophic Gastritis [17], persisting and increasing Neutrophil Infiltration is associated with Gastric Carcinogenesis [56], we also develop a novel electrochemical microfluidic chip realize precise detection of multiple biomarkers for early screening of gastric cancer [18]. We also screened out VOC biomarkers associated with early gastric cancer, advanced gastric cancer and healthy persons, developed SERS sensor to detect VOC biomarkers associated with early gastric cancer, Advanced gastric cancer and health persons, established AI model to diagnose early gastric cancer, Advanced gastric cancer and health persons, clinical test also confirms established SERS sensor can screen out early gastric cancer [23,24]. Therefore we also propose to use SERS sensor to detect VOC biomarkers associated with HP to realize precise exhaled breath diagnose for HP infection. Therefore we look for cooperation Directors of the Gastroenterology Department in hospitals, finally sign cooperation agreement via full discussion and communication, cooperation directors helped to collect exhaled samples from patients with HP infection and healthy persons without HP infection, we also used our previous established process of exhalation screening VOC biomarkers, screened out 12 VOC biomarkers, and confirmed to select 9 VOC biomarkers as standard to diagnose HP infection, it is effective, the remaining three VOC biomarkers were associated with HP resistance, which can be used to diagnose HP resistance. Based on detection data, four AI models such as DT, SVM, ANN, KNN were established, The ANN+GA model achieves an AUC of 1.00, indicating perfect classification performance [34,35].

In response to the demand for HP treatment, we also developed Oral pH sensitive GNS@ab nanoprobes for HP therapy [8], HP antibody-conjugated liposomes loaded with indocyanine green for HP therapy [9]. We found that photothermal therapy, photodynamic therapy and Sonodynamic therapy based on HP antibody-conjugated nanoprobes own obvious advantages to treat HP resistance [51,55]. Therefore, based on our previous developed Hp Ab-LiP-ICG nanoprobes for HP therapy, we start clinical test to confirm whether Hp Ab-LiP-ICG can treat effectively HP resistance. We only select 10 HP resistance patients, treatment result showed that Hp Ab-Lip-ICG combined with Ultrasound irradiation could kill HP resistance and remove killed HP. Our data also confirm that pyridine, formamide and Headecane-1,4-lactone were associated with HP resistance, which can be used to evaluate therapeutic effect of conventional clinical treatment antibiotics for HP.

In near future, we will continue to recruit patients with HP to continue to use VOC detection SERS sensor to diagnose patients with HP infection, continue to use oral Hp Ab-LiP-ICG to treat HP resistance patients, finally improve clinical translation of Exhalation screening for HP and Hp Ab-Lip-ICG for treatment of HP resistance.

Conclusion

12 VOC biomarkers were screened and confirmed that No.1-9 VOC biomarkers associated with HP infection, could be used to diagnose HP positive patients, No.10-12VOC biomarkers were associated with HP resistance, could be used to diagnose HP resistance patients. Microfludic chip SERS sensors with Fe_3O_4-silver microsphere compound was developed, which can effectively detect 12 VOC biomarkers associated with HP positive, and can confirm whether patients existed HP infection, whether patients existed HP resistance. Four AI models such as DT, SVM, ANN, KNN were established, The ANN+GA model achieves an AUC of 1.00, indicating perfect classification performance. HP Ab-Lip- ICG can be used to treat HP resistance, we will improve clinical translation of Breath screening HP and HP Antibody-conjugated Liposome-coated ICG in near future, also pay more attention on breath diagnosis and therapy of child with HP infection.

Declarations

Conflicts of interest: The authors declare no competing financial interest.

Acknowledgments: This work was supported from Project of International Cooperation and Exchanges of the National Natural Science Foundation of China (No. 82020108017), Henan Provincial Medical Science and Technology Research Plan -Major Provincial-Ministerial Jointly Funded Project (SBGJ202501009), Henan Province Zhongyuan Scholar Talent Project (No.26400510010), Innovation Group Project of National Natural Science Foundation of China (No.81921002), National Key Research and Development Program of China (No. 2017FYA0205301), Projects of Shanghai Science and Technology Commission (21DZ2203200, and No. 20142201300), and Natural Science Foundation of Shanghai (No. 22ZR1467600).

Author contributions: Huang YiXin directed and conceived this project with input from Cui Daxiang and Zhong Lan, Yang Dongmei. Huang YiXin, Xue Cuili, Wang Wei synthesized the materials, performed most of the experimental work, and wrote the draft of the manuscript. Jiang jinlei, Binyu Zhu, Yao Hu, Linjia Peng, Shengsheng Cui, Zhao Qirui, Hui Liang, Ren Zhiguang, Zhe Yu, Fangfang Xia performed the experimental data analysis. Lichen Xiang, Jesus M. de la Fuente, Fangfang Xia performed the theoretical study. Cui Daxiang, Zhong Lan, Yang Dongmei designed the project. All the authors discussed the results and contributed to the writing and revision of the manuscript.

References

1. Elbehiry A, et al. Helicobacter pylori infection: current status and future prospects on diagnostic, therapeutic and control challenges. Antibiotics (Basel). 2023; 12: 25.
2. Crowe SE. Helicobacter pylori infection. N Engl J Med. 2019; 380: 1158-1165.
3. FitzGerald R, Smith SM. An overview of Helicobacter pylori infection. Methods Mol Biol. 2021; 2283: 1-14.
4. Gravina AG, Zagari RM, De Musis C, et al. Helicobacter pylori and extragastric diseases: a review. World J Gastroenterol. 2018; 24: 3204-3221.
5. Tang X, Tay A, Benghezal M, et al. Advances in Helicobacter pylori lipopolysaccharide structure and function. FEMS Microbiol Rev. 2025; 49: fuaf034.
6. Kamboj AK, Cotter TG, Oxentenko AS. Helicobacter pylori: the past, present, and future in management. Mayo Clin Proc. 2017; 92: 599-604.
7. Tshibangu-Kabamba E, Yamaoka Y. Helicobacter pylori infection and antibiotic resistance: from biology to clinical implications. Nat Rev Gastroenterol Hepatol. 2021; 18: 613-629.
8. Hasanuzzaman M, Bang CS, Gong EJ. Antibiotic resistance of Helicobacter pylori: mechanisms and clinical implications. J Korean Med Sci. 2024; 39: e44.
9. Zhi X, Liu YL, Lin LN, et al. Oral pH-sensitive GNS@ab nanoprobes for targeted therapy of Helicobacter pylori without disturbing the gut microbiome. Nanomedicine. 2019; 20: 102019.
10. Wang RH, Song CF, Gao A, et al. Antibody-conjugated liposomes loaded with indocyanine green for oral targeted photoacoustic imaging-guided sonodynamic therapy of Helicobacter pylori infection. Acta Biomater. 2022; 143: 418-427.
11. Talley NJ, Vakil N, American College of Gastroenterology. Guidelines for the management of dyspepsia. Am J Gastroenterol. 2005; 100: 2324-2337.
12. Reshetnyak VI, Burmistrov AI, Maev IV. Helicobacter pylori: commensal, symbiont or pathogen? World J Gastroenterol. 2021; 27: 17.
13. Cardos AI, et al. Evolution of diagnostic methods for Helicobacter pylori infections: from traditional tests to high technology, advanced sensitivity and discrimination tools. Diagnostics (Basel). 2022; 12: 23.
14. Zhou C, Jiang J, Huang S, et al. An ingestible near-infrared fluorescence capsule endoscopy for specific gastrointestinal diagnoses. Biosens Bioelectron. 2024; 257: 116209.
15. Zheng Y, Wang K, Zhang JJ, et al. Simultaneous quantitative detection of Helicobacter pylori based on a rapid and sensitive testing platform using quantum dots-labeled immunochromatographic test strips. Nanoscale Res Lett. 2016; 11: 62.
16. Gui C, Wang K, Li C, Dai X, Cui DX. A CCD-based reader combined with CdS quantum dot-labeled lateral flow strips for ultrasensitive quantitative detection of CagA. Nanoscale Res Lett. 2014; 9: 57.

17. Chen J, Wang W, Zhang T, et al. Differential expression of phospholipase C epsilon 1 is associated with chronic atrophic gastritis and gastric cancer. PLoS One. 2012; 7: e47563.

18. Xie Y, Zhi X, Su HC, et al. A novel electrochemical microfluidic chip combined with multiple biomarkers for early diagnosis of gastric cancer. Nanoscale Res Lett. 2016; 10: 477.

19. Sharma A, Kumar R, Varadwaj P. Smelling the disease: diagnostic potential of breath analysis. Mol Diagn Ther. 2023; 27: 321-347.

20. Atherton JC, Spiller RC. The urea breath test for Helicobacter pylori. Gut. 1994; 35: 723-725.

21. Saalberg Y, Wolff M. VOC breath biomarkers in lung cancer. Clin Chim Acta. 2016; 459: 5-9.

22. Zhang J, et al. Breath volatile organic compound analysis: an emerging method for gastric cancer detection. J Breath Res. 2021; 15: 24.

23. Chen Y, Zhang Y, Pan F, et al. Breath analysis based on surface-enhanced Raman scattering sensors distinguishes early and advanced gastric cancer patients from healthy persons. ACS Nano. 2016; 10: 8169-8179.

24. Aslam MA, Xue CL, Chen YS, et al. Breath analysis-based early gastric cancer classification from deep stacked sparse autoencoder neural network. Sci Rep. 2021; 11: 4014.

25. Xue C, et al. Development of exhaled breath diagnosis sensors for rapid identification of COVID-19 patients. Nano Biomed Eng. 2021; 13: 225-228.

26. Xue CL, et al. Intelligent COVID-19 screening platform based on breath analysis. J Breath Res. 2023; 17: 11.

27. Xue C, Yi C, Zhang L, et al. Unlocking pan-cancer detection via phenyl-β-D-glucuronide-induced breath analysis. Cell Biomater. 2026; 2: 100421.

28. Ulanowska A, et al. Determination of volatile organic compounds in human breath for Helicobacter pylori detection by SPME-GC/MS. Biomed Chromatogr. 2011; 25: 391-397.

29. Zhang YN, Yao HZ, Xue CL, et al. Au nanostars coated with a thin film of MIL-100(Fe) for SERS-based sensing of volatile organic compound indicators in saliva. ACS Appl Nano Mater. 2024; 7: 2735-2743.

30. Shipe ME, et al. Developing prediction models for clinical use using logistic regression: an overview. J Thorac Dis. 2019; 11: S574-S584.

31. Kavitha MS, Shanthini J, Sabitha R. ECM-CSD: an efficient classification model for cancer stage diagnosis in CT lung images using FCM and SVM techniques. J Med Syst. 2019; 43: 9.

32. Xiang MY, Liu YM, Yang ZY, et al. A flexible single-sensor MEMS e-nose with dual-temperature modulation for VOC classification and breath-based silent communication. Small. 2025; 21: 2505098.

33. Soumaya Z, et al. The detection of Parkinson disease using the genetic algorithm and SVM classifier. Appl Acoust. 2021; 171: 10.

34. Huang S, Zhang L, Liu X. Bioinformatics approach to identifying molecular targets of isoliquiritigenin affecting chronic obstructive pulmonary disease: a machine learning pharmacology study. Int J Mol Sci. 2025; 26: 3907.

35. Zhu X, Li Y, Gu N. Application of artificial intelligence in the exploration and optimization of biomedical nanomaterials. Nano Biomed Eng. 2023; 15: 342-353.

36. Chen MR, Cui DX, Haick H, Tang N. Artificial intelligence-based medical sensors for healthcare system. Adv Sens Res. 2024; 3: 2300009.

37. Wang JH, Zhou C, Wang W, et al. A multimodal deep learning model for detecting endoscopic images of near-infrared fluorescence capsules. Biosens Bioelectron. 2025; 278: 117251.

38. Wang JH, Liu G, Zhou C, et al. Application of artificial intelligence in cancer diagnosis and tumor nanomedicine. Nanoscale. 2024; 16: 14213-14246.

39. Chang J, Zhang A, Huang ZC, et al. Monodisperse Au@Ag core-shell nanoprobes with ultrasensitive SERS activity for rapid identification and Raman imaging of living cancer cells. Talanta. 2019; 198: 45-54.

40. Feliu N, Hassan M, Rico EG, et al. SERS quantification and characterization of proteins and other biomolecules. Langmuir. 2017; 33: 9711-9730.

41. Hu CY, Yang DP, Xu K, et al. Ag@BSA core/shell microspheres as an electrochemical interface for sensitive detection of urinary retinol-binding protein. Anal Chem. 2012; 84: 10324-10331.

42. Zhang XQ, Guo Q, Cui DX. Recent advances in nanotechnology applied to biosensors. Sensors (Basel). 2009; 9: 1033-1053.

43. Huang P, Li ZM, Lin J, et al. Photosensitizer-conjugated magnetic nanoparticles for in vivo simultaneous magnetofluorescent imaging and targeting therapy. Biomaterials. 2011; 32: 3447-3458.

44. Wang C, Bao CC, Liang SJ, et al. HAI-178 antibody-conjugated fluorescent magnetic nanoparticles for targeted imaging and simultaneous therapy of gastric cancer. Nanoscale Res Lett. 2014; 9: 274.

45. Gao G, Wu HX, Gao WJ, et al. Preparation of FeCO3-Fe3O4 nanoparticles and flower-like assemblies via a one-step hydrothermal method. CrystEngComm. 2011; 13: 6950-6954.

46. Huang P, Yang DP, Zhang CL, et al. Protein-directed one-pot synthesis of Ag microspheres with good biocompatibility and enhancement of radiation effects on gastric cancer cells. Nanoscale. 2011; 3: 3623-3626.

47. Wang XS, Yang DP, Huang P, et al. Hierarchically assembled Au microspheres and sea urchin-like architectures: formation mechanism and SERS study. Nanoscale. 2012; 4: 7766-7772.

48. Yang DP, Chen SH, Huang P, et al. Bacteria-template synthesized silver microspheres with hollow and porous structures as excellent SERS substrate. Green Chem. 2010; 12: 2038-2042.

49. Gao G, Wang K, Huang P, et al. Superparamagnetic Fe3O4-Ag hybrid nanocrystals as a potential contrast agent for CT imaging. Cryst Eng Comm. 2012; 14: 7556-7559.

50. Wang JH, Liu G, Zhou C, et al. Application of artificial intelligence in cancer diagnosis and tumor nanomedicine. Nanoscale. 2024; 16: 14213-14246

51. Jiang J, Cui X, Huang Y, et al. Advances and prospects in integrated nano-oncology. Nano Biomed Eng. 2024; 16: 152-187.

52. Yuan C, Adeloye D, Lukt T, et al. The global prevalence of and factors associated with Helicobacter pylori infection in children: a systematic review and meta-analysis. Lancet Child Adolesc Health. 2022; 6: 185-194.

53. Queiroz DM, Rocha AM, Crabtree JE. Unintended consequences of Helicobacter pylori infection in children in developing countries: iron deficiency, diarrhea, and growth retardation. Gut Microbes. 2013; 4: 494-504.

54. Xu C, Wu Y, Xu S. Association between Helicobacter pylori infection and growth outcomes in children: a meta-analysis. Helicobacter. 2022; 27: e12861.

55. Li M, Gong Y, Chen T, et al. Nanobiomaterials-based sonodynamic therapy for treatment of Helicobacter pylori infections: a review. Nano Biomed Eng. 2024; 16: 525-541.

56. Fu HL, Ma Y, Yang M, et al. Persisting and increasing neutrophil infiltration associates with gastric carcinogenesis and E-cadherin downregulation. Sci Rep. 2016; 6: 29762.

Supporting data

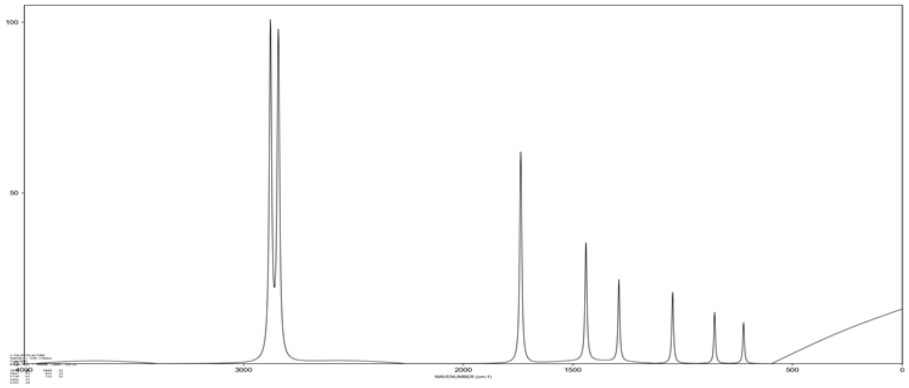

Figure S1: Raman spectra of No.12 biomarker Headecane-1, 4-lactone.

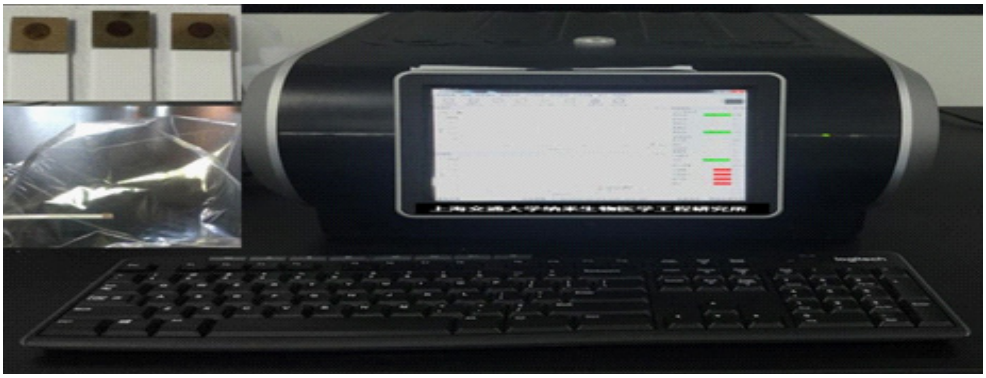

Figure S2: Model machine for VOC detection.

This prototype has been evaluated and verified by a third-party medical device assessment agency.

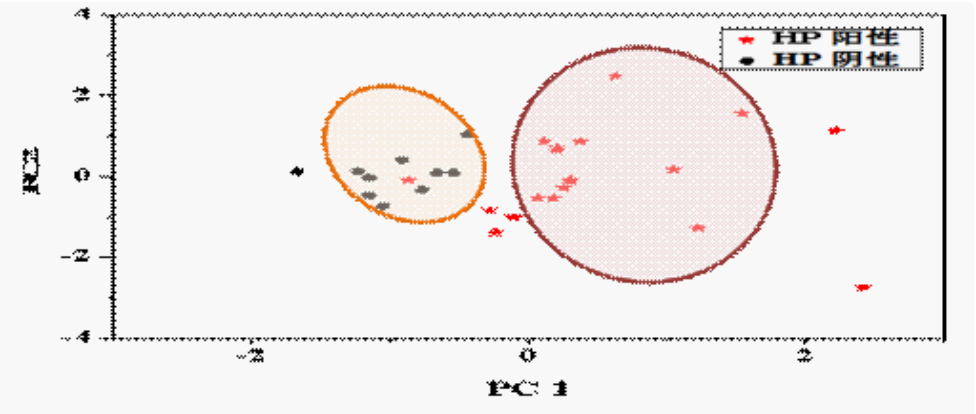

Figure S3: Result of detection of HP positive and HP negative.

Table S1:

Peak	VOC biomarker	Relative concentrationa		
		HP negative	HP resistance	HP without resistance
1	n-hexane	0.174±0.0822	6.2±0.193	6.3±0.184
2	ethyl acetate	0.145±0.0391	4.6±0.134	2.5±0.132
3	2-methyl-1-propanol	0.0581±0.0177	3.4±0.421	3.4±0.510
4	alcohol	0.0265±0.0352	5.2±0.119	4.8±0.121
5	toluene	0 ± 0	4.1±0.510	3.9±0.428
6	1-Propanol	0.0438±0.0211	5.8±0.121	5.9±0.131
7	hexanal	0 ± 0	4.7 0±0.212	4.9 0±0.311
8	o-xylene	0.0241 0±0.0134	6.3±0.311	5.4±0.324
9	pyridine	0 ± 0	7.1±0.440	3.6±0.324
10	nonanal	0 ± 0	8.2±1.21	0.7±0.242
11	formamide	0 ± 0	7.6±1.28	0.4±0.11
12	Headecane-1,4-lactone	0 ± 0	9.2±1.33	0 ± 0

Table S2:

Peak	VOC biomarker	Concentration (10 patients' Average data)	
		Before Therapy	After Therapy for 1 week
1	n-hexane	6.2	0
2	ethyl acetate	4.6	0
3	2-methyl-1-propanol	3.4	0
4	alcohol	5.2	0.02
5	toluene	4.3	0
6	1-Propanol	5.8	0.03
7	hexanal	4.7	0
8	o-xylene	6.6	0.024
9	pyridine	7.5	0.012
10	nonanal	8.3	0
11	formamide	8.6	0
12	Headecane-1,4-lactone	9.2	0

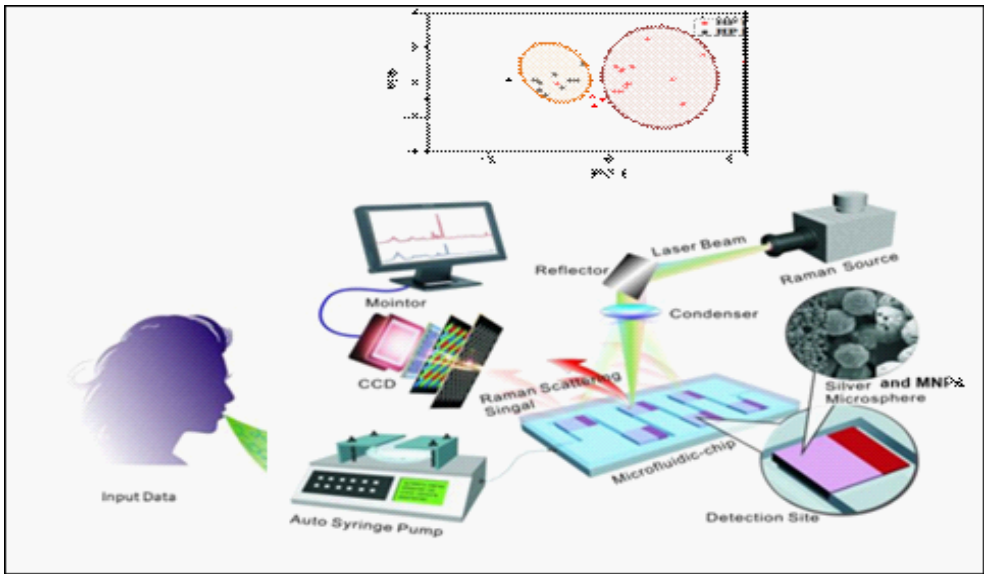

Figure S3: Schematic diagrams of SERS sensor and overview of the processes involved in the breath analysis.

HP-Ab-Lip-ICG synthesis

1,2-Dioctadecanoyl-sn glycero-3-phophocholine (DSPC) and Cholest-5-en-3β-ol (CHO HP) were purchased from Aiweituo Pharmaceutical Technology Co., Ltd. (Shanghai, China). 1,2-Distearoyl-sn glycero-3-phosphoethanolamine-N-[maleimide(polyethyleneglycol)] (DSPE-PEG-Mal) was bought from Jiuai Biotechnology Co., Ltd. (Shanghai, China). ICG was purchased from Yinuokai Technology Co., Ltd. (Beijing, China). Monoclonal mouse anti-H. pylori antibody (HpAb, H01A43) was obtained from Riogene Biotech Co.,

HP-Ab-Lip-ICG was prepared based on our reported method as follow:

Wang, RH, Song, CF, Gao, A, etal. Antibody-conjugated liposomes loaded with indocyanine green for oral targeted photoacoustic imaging-guided sonodynamic therapy of Helicobacter pylori infection. Acta Biomaterialia. 2022; 143: 418-427.